Molecular Biology of the Cell
Vol. 17, 1620–1631, April 2006

Rgf1p Is a Specific Rho1-GEF That Coordinates Cell Polarization with Cell Wall Biogenesis in Fission Yeast

Patricia García, Virginia Tajadura, Ignacio García, and Yolanda Sánchez

Instituto de Microbiología Bioquímica, CSIC/Universidad de Salamanca and Departamento de Microbiología y Genética, Universidad de Salamanca, Campus Miguel de Unamuno, 37007 Salamanca, Spain

Submitted October 7, 2005; Revised December 16, 2005; Accepted January 10, 2006
Monitoring Editor: Anne Ridley

Rho1p regulates cell integrity by controlling the actin cytoskeleton and cell wall synthesis. We have identified a new GEF, designated Rgf1p, which specifically regulates Rho1p during polarized growth. The phenotype of *rgf1* null cells was very similar to that seen after depletion of Rho1p, 30% of cells being lysed. In addition, *rgf1*$^+$ deletion caused hypersensitivity to the antifungal drug Caspofungin and defects in the establishment of bipolar growth. *rho1*$^+$, *but* none of the other GTPases of the Rho-family, suppressed the *rgf1*Δ phenotypes. Moreover, deletion of *rgf1*$^+$ suppressed the severe growth defect in *rga1*$^+$ null mutants (a Rho1-GAP, negative regulator). Rgf1p and Rho1p coimmunoprecipitated and overexpression of *rgf1*$^+$ specifically increased the GTP-bound Rho1p; it caused changes in cell morphology, and a large increase in β(1,3)-glucan synthase activity. These effects were similar to those elicited when the hyperactive *rho1-G15V* allele was expressed. A genetic relationship was observed between Rgf1p, Bgs4p (β[1,3]-glucan synthase), and Pck1p (protein kinase C [PKC] homologue); Bgs4p and Pck1p suppressed the hypersensitivity to Caspofungin in *rgf1*Δ mutants. Rgf1p localized to the growing ends and the septum, where Rho1, Pck1p, and Bgs4p are known to function. Our results suggest that Rgf1p probably activates the Rho functions necessary for coordinating actin deposition with cell wall biosynthesis during bipolar growth, allowing the cells to remodel their wall without risk of rupture.

INTRODUCTION

Fission yeast cells are rod-shaped and grow in a polarized manner at the cell ends. Immediately after cell division, the daughter cells initiate growth in a monopolar manner from the cell end that preexisted before cell division (the old end). After a point in G2, cells initiate growth from the new end (the end created by cell division) in a process known as new end take off (NETO), so that they grow in a bipolar mode up to mitosis (Mitchison and Nurse, 1985; Hayles and Nurse, 2001). Fission yeast is a useful model system for studying cell wall biosynthesis and how this fits in the complex morphogenetic processes required for the cell shape to be attained.

The *Schizosaccharomyces pombe* cell wall consists mainly of three polysaccharides, β(1,3)-glucan, α(1,3)-glucan, and galactomannoproteins, all of which form a large complex. Their coordinated synthesis represents an essential step in the assembly of a functional cell wall to ensure cell integrity (for a review, see Duran and Perez, 2004). Among the polysaccharides, β(1,3)-glucans are the most prevalent (50–54% of the wall) and it is generally accepted that they are the main structural components responsible for cell wall rigidity (Manners and Meyer, 1977). β(1,3)-glucan is the first polymer to be synthesized in *S. pombe* regenerating protoplasts (Osumi *et al.*, 1989) and in the spore wall (Martin *et al.*, 2000) and hence the regulation of this polysaccharide may be a key step in the sequential assembly of the other cell wall components. The enzymatic system that catalyzes the synthesis of this polysaccharide is β(1,3)-glucan synthase (GS). GS is composed of at least two fractions: the catalytic moiety of the enzyme and the regulatory component. The catalytic subunit of GS is encoded by at least four genes: *cps1*$^+$/*bgs1*$^+$ (Le Goff *et al.*, 1999; Liu *et al.*, 2000b, 2002; Cortes *et al.*, 2002), *bgs2*$^+$ (Martin *et al.*, 2000; Liu *et al.*, 2000a), *bgs3*$^+$ (Martin *et al.*, 2003), and *bgs4*$^+$ (Cortes *et al.*, 2005). All of them code for essential proteins at different stages in the cellular life cycle. In addition to the catalytic subunit, the small GTP-binding protein Rho1p is an essential regulatory subunit (Arellano *et al.*, 1996; Nakano *et al.*, 1997). Rho1 acts as a binary switch by cycling between an inactive GDP-bound and an active GTP-bound conformational state. Rho1p stimulates GS in its GTP-bound prenylated form, providing a rationale for an understanding of the mechanism through which the cell can switch β(1,3)-glucan synthesis on and off by interconverting the GDP and GTP forms of Rho1p.

To maintain intracellular osmolarity and to produce cell shapes other than spheres, cell wall expansion must be focused on particular regions. *S. pombe* uses both microtubules and the actin cytoskeleton for this purpose (for reviews, see Yarm *et al.*, 2001; Chang and Verde, 2004; Gachet *et al.*, 2004). It has been proposed that microtubules (MTs) would act to localize key proteins involved in setting up polarized growth or to localize secretion, or even to localize actin itself to the cortex. Actin is strictly required for cell growth and is assembled in three types of structures: actomyosin rings, actin cables, and actin patches. Both cables and patches are reorganized during the cell cycle and are focused around the areas of cell growth (Marks and Hyams, 1985). The cables serve as trackways along which both actin patches (Pelham and Chang, 2001) and presumably also myosin motors with their associated cargos move to the poles or the equator for cell growth (Win *et al.*, 2001). Actin patches are dense membrane-associated structures possibly

This article was published online ahead of print in *MBC in Press* (http://www.molbiolcell.org/cgi/doi/10.1091/mbc.E05–10–0933) on January 18, 2006.

Address correspondence to: Yolanda Sánchez (ysm@usal.es).

involved in localized cell wall synthesis. In fission yeast regenerating protoplasts, their localization coincides precisely with active sites of cell wall deposition (Kobori *et al.*, 1989).

Rho1p provides a link between polarized growth and cell wall biosynthesis (Arellano *et al.*, 1997; Nakano *et al.*, 1997), and it belongs to a family of small GTPases that are key regulators in morphogenesis, polarity, movement, and division processes (reviewed in Jaffe and Hall, 2005). The fission yeast Rho family includes Cdc42p and Rho1p through Rho5p. Rho1p localizes to sites of polarized growth, the cell poles, and the septum (Arellano *et al.*, 1997; Nakano *et al.*, 1997) and activates the abovementioned cell wall-synthesizing enzyme GS (Arellano *et al.*, 1996); Rho1 also regulates the organization of F-actin patches (Arellano *et al.*, 1997), and it binds directly to the PKC family of protein kinases, Pck1p and Pck2p, functioning as a positive regulator of these (Arellano *et al.*, 1999b; Sayers *et al.*, 2000). However, little is known about the proteins that turn Rho1p on and off in the cell. Rho GTPase regulators such as GEFs (GDP-GTP exchange factors) modify the nucleotide-bound state of the GTPase and contain protein–protein interaction domains that could be important for GTPase localization, activation, and stabilization, and thus for interaction with its effectors (Gulli and Peter, 2001; Rossman *et al.*, 2005). *S. pombe* contains seven genes bearing a Rho-GEF domain: *scd1*$^+$, *gef1*$^+$, *gef2*$^+$, *gef3*$^+$, *rgf1*$^+$, *rgf2*$^+$, and *rgf3*$^+$ (Iwaki *et al.*, 2003). Of these, *scd1*$^+$ and *gef1*$^+$ are Cdc42p-specific GEF(s) and Rgf3p has been described to function as a GEF for Rho1p. *rgf3*$^+$ is an essential gene and regulates cell wall β-glucan biosynthesis through the GTPase Rho1p, in particular during cytokinesis (Tajadura *et al.*, 2004). Previous studies have shown that Rho1p depletion causes cell death that cannot be prevented by an osmotic stabilizer (Arellano *et al.*, 1997). However, Rgf3p depletion was prevented by 1.2 M sorbitol (Tajadura *et al.*, 2004). This intriguing phenomenon suggests that in the absence of Rgf3p, but in the presence of an osmotic support, Rho1p could be activated in some other way. Accordingly, we hypothesized that this function of Rho1p would be regulated by other GEF(s) (Iwaki *et al.*, 2003). Here we demonstrate that Rgf1p specifically activates Rho1p. Our data support a model in which Rgf1p would coordinate actin deposition at polarized sites with cell wall biosynthesis, allowing the cells to remodel their wall without risk of rupture.

MATERIALS AND METHODS

Media, Reagents, and Genetics

The genotypes of the *S. pombe* strains used in this study are listed in Table 1. The complete yeast growth medium (YES), selective medium (MM) supplemented with the appropriate requirements and sporulation medium (MEA) have been described elsewhere (Moreno *et al.*, 1991). Caspofungin (Csp; Deresinski and Stevens, 2003) was stored at −20°C in a stock solution (2.5 μg/ml) in H_2O and was added to the media at the corresponding final concentration after autoclaving. Crosses were performed by mixing appropriate strains directly on MEA plates. Recombinant strains were obtained by tetrad analysis. For overexpression experiments using the *nmt1* promoter, cells were grown in EMM containing 15 μM thiamine up to the logarithmic phase. Then, the cells were harvested, washed three times with water, and inoculated in fresh medium (without thiamine) at an OD_{600} = 0.01.

Table 1. *S. pombe* strains used in this work

Strains	Genotypes
YSM180	h$^-$ 972
PN22	h$^-$ *leu1-32*
GI 1	h$^+$ *leu1-32, ehs2-1*
YS64	h$^-$ *leu1-32 ade6M210 ura4D-18 his3D1*
HVP54	h$^-$ *leu1-32 ade6M210 ura4D-18*
YS165	h$^+$/h$^-$ *leu1-32/leu1-32 ade6M210/ade6M216 ura4D-18/ura4D-18 his3D1/his3D1*
VT14	h$^-$ *leu1-32 ade6M210 ura4D-18 his3D1rgf1::his3*$^+$
VT18	h$^+$ *leu1-32 ade6M210 ura4D-18 his3D1rgf1::his3*$^+$
PG65	h$^-$ *leu1-32 ade6M210 ura4D-18 his3D1rgf1::kanMX6*
PG40	h$^-$ *rgf1::his3 his3D1 leu1-32 ade6M210 ura4D-18 leu1*$^+$*: rgf1*$^+$*-GFP*
PG92	h$^-$ *leu1-32 ade6M210 ura4D-18 his3D1rgf1::his3*$^+$*crn1*$^+$*-GFP:KanMX6*
JCR962	h$^+$ *leu1-32 ura4D-18 ade6 crn1*$^+$*-GFP:KanMX6*
KNG101	h$^+$/h$^-$ *rga1::ura4*$^+$ *leu1-32 ura4-D18 ade6M216/rga1*$^+$ *leu1-32 ura4-D18 ade6M210*
PG72	h$^+$/h$^-$ *rga1::ura4*$^+$ *rgf1::kanMX6 leu1-32 ura4-D18 ade6M216/rga1*$^+$ *rgf1*$^+$ *leu1-32 ura4-D18 ade6M210*
PG73-1c	*rga1::ura4*$^+$ *rgf1::kanMX6 leu1-32 ura4-D18 ade6M216*
PG74-2b	*rga1::ura4*$^+$ *leu1-32 ura4-D18 ade6M216*
PG75-4c	*rga1*$^+$ *leu1-32 ura4-D18 ade6M210*
PG76-5a	*rgf1::kanMX6 leu1-32 ura4-D18 ade6M216*
MS168	h$^-$ *leu1-32 ura4D-18 cdc10-129*
PG88	h$^+$ *leu1-32 ura4D-18 cdc10-129rgf1::his3*$^+$
NG669	h$^-$ *leu1-32 ura4D-18 cdc25-22*
PG43	h$^+$ *leu1-32 ura4D-18 cdc25-22rgf1::his3*$^+$
YSM373	h$^+$/h$^-$ *leu1-32/leu1-32 ade6M210/ade6M216, rgf3::ura4*$^+$*/rgf3*$^+$ *his3D1/his3D1 ura4D-18/ura4D-18*
VT128	h$^-$ *leu1-32 ade6M210 ura4D-18, his3DI leu1*$^+$*: EGFP- rgf3*$^+$
PPG217	h$^-$ *leu1-32 ade6M210 ura4D-18 his3D1 rho1::ura4*$^+$ +pREP41X-*rho1*
JCR132	h$^-$ *leu1-32 cwg1-1*
PG76	h$^+$ *rgf1::kanMX6*
PG82	h$^-$ *cwg1-1 rgf1::kanMX6*

Plasmid and DNA Manipulations

pYS8, containing the *rgf1* ORF, was obtained by inserting a 7-kb EcoRI fragment from cosmid C645 into pAU-KS (Tajadura *et al.*, 2004). An XhoI-NotI fragment from pYS8 (containing the 7-kb EcoRI fragment) was subcloned into the XhoI-NotI sites of pAL-KS, thus affording pAL-*rgf1*$^+$. To tag Rgf1p at the C-terminus with enhanced green fluorescent protein (EGFP) and with the triple repeat of the influenza virus hemagglutinin (HA) epitope (Craven *et al.*, 1998), pAL-*rgf1*$^+$ was modified by site-directed mutagenesis. We destroyed the NotI site at the multiple cloning site and created a NotI site by site-directed mutagenesis just before the TAA stop codon of *rgf1*$^+$ (pGR41). The GFP and HA epitopes were inserted in-frame at the NotI site of pGR41. pGR45 (pAL-*rgf1*$^+$*-GFP*) and pGR46 (pAL-*rgf1*$^+$*-HA*) fully complemented the *rgf1*Δ phenotypes. Strain PG40, with the *rgf1*$^+$*-GFP* integrated under its own promoter, was constructed by subcloning the *rgf1*$^+$ tagged with GFP (from plasmid pAL-*rgf1-GFP*) into the integrative vector pIJ148, resulting in pIJ148-*rgf1*$^+$*-GFP* (pGR49). This plasmid was cut with Eco47III and integrated into the *leu1* locus of strain VT14. The *nmt*1 promoter-containing vectors pREP3X and pREP41X (Forsburg and Sherman, 1997) were used to overexpress *rho1*$^+$ to *rho5*$^+$, *cdc42*$^+$, and *rgf3*$^+$. All GTPases of the Rho family were tagged with two HA epitopes at the 5′ end (Calonge *et al.*, 2003). The *rho* overexpression plasmids were kindly provided by P. Perez and P. M. Coll (Instituto de Microbiologia Bioquimica, Salamanca, Spain). pAL-*bgs1*$^+$, pAL-*bgs2*$^+$, pAL-*bgs3*$^+$, and pAL-*bgs4*$^+$ multicopy plasmids were used to overexpress the β-GS catalytic subunits, each with their own promoter. pAL-*bgs1*$^+$ was kindly provided by J. C. Cortes and J. C. Ribas (Cortes *et al.*, 2002). pAL-*bgs2*$^+$, pAL-*bgs3*$^+$ and pAL-*bgs4*$^+$ have been described previously (Martin *et al.*, 2000, 2003; Cortes *et al.*, 2005). To overexpress *rgf1*$^+$, an XhoI-SmaI fragment containing the *rgf1*$^+$ gene tagged with the HA epitope from plasmid pGR46 was ligated into the XhoI-SmaI sites of plasmid pREP41X (pGR57) and pREP3X (pGR58). pGR33 is pREP3X with an XhoI-SmaI fragment containing the *rgf1*$^+$ ORF without the HA tag.

Rgf1 Deletion

The *rgf1::his3* disruption construct was obtained in a two-step process. The 3′-flanking region (nt 4004–5350) was obtained by PCR, inserting SalI and ApaI sites into the same sites of the SK-*his3*$^+$ vector to yield pVT16. Then, a PCR fragment of the 5′ end of *rgf1*$^+$ (nt −1490 to −62) carrying BamHI and NotI sites at the ends was digested with BamHI, treated with Klenow, and then digested with NotI and ligated into the SmaI and NotI sites of pVT16 to yield pVT2. Plasmid pVT2 was digested with ApaI and NotI, and the linear

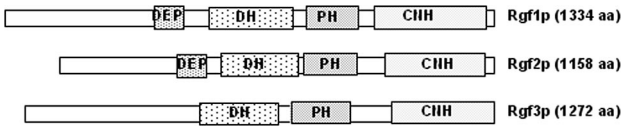

Figure 1. Comparison of structural features of Rgf1, Rgf2, and Rgf3 analyzed by the SMART program (Letunic *et al.*, 2002; http://smart.embl-heidelberg.de/). Domains are indicated: CNH, citron homology domain; DH, Dbl homology domain conserved among GEFs for Rho/Rac/Cdc42-like GTPases; PH, pleckstrin homology domain; DEP, domain of unknown function present in signaling proteins that contain PH, RasGEF, RhoGEF, RhoGAP, RGS, and PDZ domains.

DNA inserted was used to transform a diploid and a haploid strain (YS165 and YS64, respectively). Correct deletion of the *rgf1*$^+$ ORF was confirmed by PCR analysis using the following oligonucleotides: M22 (5′-GTGTTCGCTAATTGCGC-3′) into the *his3*$^+$ gene and R23-e (5′-CAAGGGTATGTGGTCTGG-3′) downstream from the nt 5350 and therefore external to the deletion cassette. A diploid strain heterozygous for the *rgf1*::*his3*$^+$ allele was subjected to tetrad analysis. *his*$^+$/*his*$^-$ segregation in tetrads was regular, indicating that *rgf1*$^+$ is not essential for vegetative growth. Gene replacement was also confirmed by genomic Southern blotting of a tetrad (unpublished data). To make the *rgf1*::*kan* disruption construct (pGR59), pVT2 was cut with SalI and SpeI (to eliminate the *his3* marker) and replaced it by the *kanMX6* gene from pFA6a-kanMX6, (Bähler *et al.*, 1998). Plasmid pGR59 was digested with ApaI and NotI and the linear DNA containing the cassette was used transform a haploid strain (YS64). *rgf1*::*kan*^{R} disruptants were selected as Kanamicin-resistant and Caspofungin-hypersensitive. *cdc25-2 rgf1*Δ and *cdc10-129 rgf1*Δ mutants were obtained by genetic crosses; the offspring were analyzed for *cdc* (ts phenotype) and for *rgf1*Δ kanamicin resistance and Caspofungin hypersensitivity. *cwg1-1 rgf1*Δ mutants were obtained by genetic cross of *cwg1-1* (JCR132) and *rgf1*Δ (PG76) strains and selected from tetrads where NPD (nonparental ditypes) were produced.

Immunoprecipitation

Rho1-GST (in pREP-KZ; a gift from P. Perez and P. M. Coll; Calonge *et al.*, 2003) and pREP41X-*rgf1HA* (pGR57) were used to cotransform *leu1-32 ura4D18 S. pombe* cells and protein expression was induced by growing the cells in the absence of thiamine for 18 h. Extracts from 2×10^8 cells expressing GST-Rho1p/Rgf1p-HA, GST/Rgf1p-HA, and GST-Rho1p/Rgf1p were obtained using 200 μl of lysis buffer (50 mM Tris, pH 7.5, 2 mM EDTA, 137 mM NaCl, 0.5% NP-40, 10% glycerol containing 100 μM *p*-amino-phenyl methanesulfonyl fluoride, leupeptin, and aprotinin). The beads were washed four times with lysis buffer and then resuspended in sample buffer and subjected to 7.5% SDS-PAGE. The separated proteins were transferred electrophoretically to an Immobilon-P membrane (Millipore, Bedford, MA) and blotted to detect Rgf1p-HA with 1:5000 diluted 12CA5 monoclonal antibody (mAb) as primary antibody and the enhanced chemiluminescence detection kit (Amersham Biosciences, Piscataway, NJ). Total Rgf1p-HA levels were monitored in whole cell extracts (50 μg of total protein) and used directly for Western blot.

Pulldown Assay for GTP-bound Rho Proteins

The expression vector pGEX-C21RBD (rhotekin-binding domain; Reid *et al.*, 1996) was used to transform *Escherichia coli* cells. The fusion protein was produced according to the manufacturer's instructions and immobilized on glutathione-Sepharose 4B beads (Amersham). After incubation, the beads were washed several times, and the bound proteins were analyzed by SDS-PAGE and stained with Coomassie. The amount of GTP-bound Rho proteins was analyzed using the Rho-GTP pulldown assay modified from Ren *et al.* (1999). Briefly, wild-type, *rgf1*$^+$-overexpressing, and *rgf1*Δ mutant cells were transformed with either pREP3X-*HArho1*$^+$ or pREP3X-*HArho4*$^+$ and grown for 18 h in minimal medium without thiamine. Extracts from 10^8 cells were obtained as described previously (Arellano *et al.*, 1997), using 500 μl of lysis buffer (50 mM Tris, pH 7.5, 20 mM NaCl, 0.5% NP-40, 10% glycerol, 0.1 μM dithiothreitol, 1 mM NaF, 2 mM $MgCl_2$, containing 100 μM *p*-aminophenyl methanesulfonyl fluoride, leupeptin, and aprotinin). GST-RBD fusion protein, 100 μg, coupled to glutathione-agarose beads was used to immunoprecipitate 1.5 mg of the cell lysates. The extracts were incubated with GST-RBD beads for 2 h. The beads were washed with lysis buffer four times, and bound proteins were blotted against 1:2000-diluted 12CA5 mAb as primary antibody to detect HA-Rho1p or HA-Rho4p. The total amounts of HA-Rho1p or HA-Rho4p levels were monitored in whole-cell extracts (10 μg of total protein), which were used directly for Western blot and were developed with 12CA5 mAb. Immunodetection was accomplished using the ECL detection kit (Amersham Biosciences).

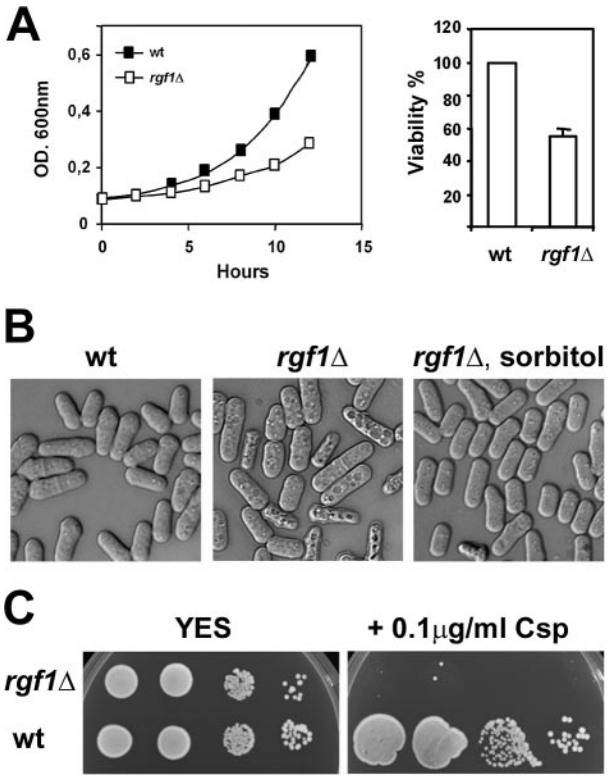

Figure 2. Growth phenotypes of *rgf1*Δ null cells. (A) Left, growth curves of *rgf1*Δ cells (VT14) and the corresponding isogenic wild-type cells (HVP54). Log-phase cells grown at 28°C were diluted to the same optical density and further grown in YES medium. Right, percentage of colony forming units (cfu) of the mutant *rgf1*Δ compared with that of the wild-type isogenic strain. Cells prepared as above were diluted and counted, and the same number of cells were plated on YES medium and incubated for 3 d at 28°C. (B) Morphology of *rgf1*Δ mutant. Differential interference contrast (DIC) micrographs of *S. pombe* wild type (HVP54) and *rgf1*Δ (VT14) grown in YES liquid medium at 28°C; in right panel, *rgf1*Δ cells were grown in the presence of 1.2 M sorbitol for 6 h. (C) *rgf1*Δ mutant cells are hypersensitive to Caspofungin (Csp). Equal number of wild-type and *rgf1*Δ cells were diluted and (4×10^4, 2×10^4, 2×10^2, and 2×10^1 cells, respectively) were spotted onto YES plates with or without 0.1 μg/ml Csp (CANCIDAS). Colony formation was analyzed following 2–3 d of incubation at 28°C.

Cell Wall Analyses

Enzyme preparations and GS assays were performed basically as described previously (Martin *et al.*, 2000). Cell extracts were obtained from early log-phase cells grown in MM as indicated for each case. Standard GS assays contained 15–25 μg protein of enzyme extract (3–5 mg protein/ml) in a total volume of 40 μl and the reaction was incubated at 30°C for 60–90 min. All reactions were carried out in duplicate and the values were calculated from three independent cell cultures. One unit of activity was measured as the amount that catalyzes the incorporation of 1 μmol of substrate (UDP-D-glucose) min^{-1} at 30°C.

Microscopy Techniques

The localization of Rgf1p-GFP, Crn1p-GFP, and Atb2p-GFP was visualized in living cells. For Calcofluor staining, exponentially growing *S. pombe* cells were harvested, washed once, and resuspended in water with Calcofluor (Cfw) at a final concentration 20 μg/ml for 5 min at room temperature. After washing with water, cells were observed under a DMRXA microscope (Leica, Wetzlar, Germany). Actin staining was performed using AlexaFluor 488-phalloidin (Molecular Probes, Eugene, OR).

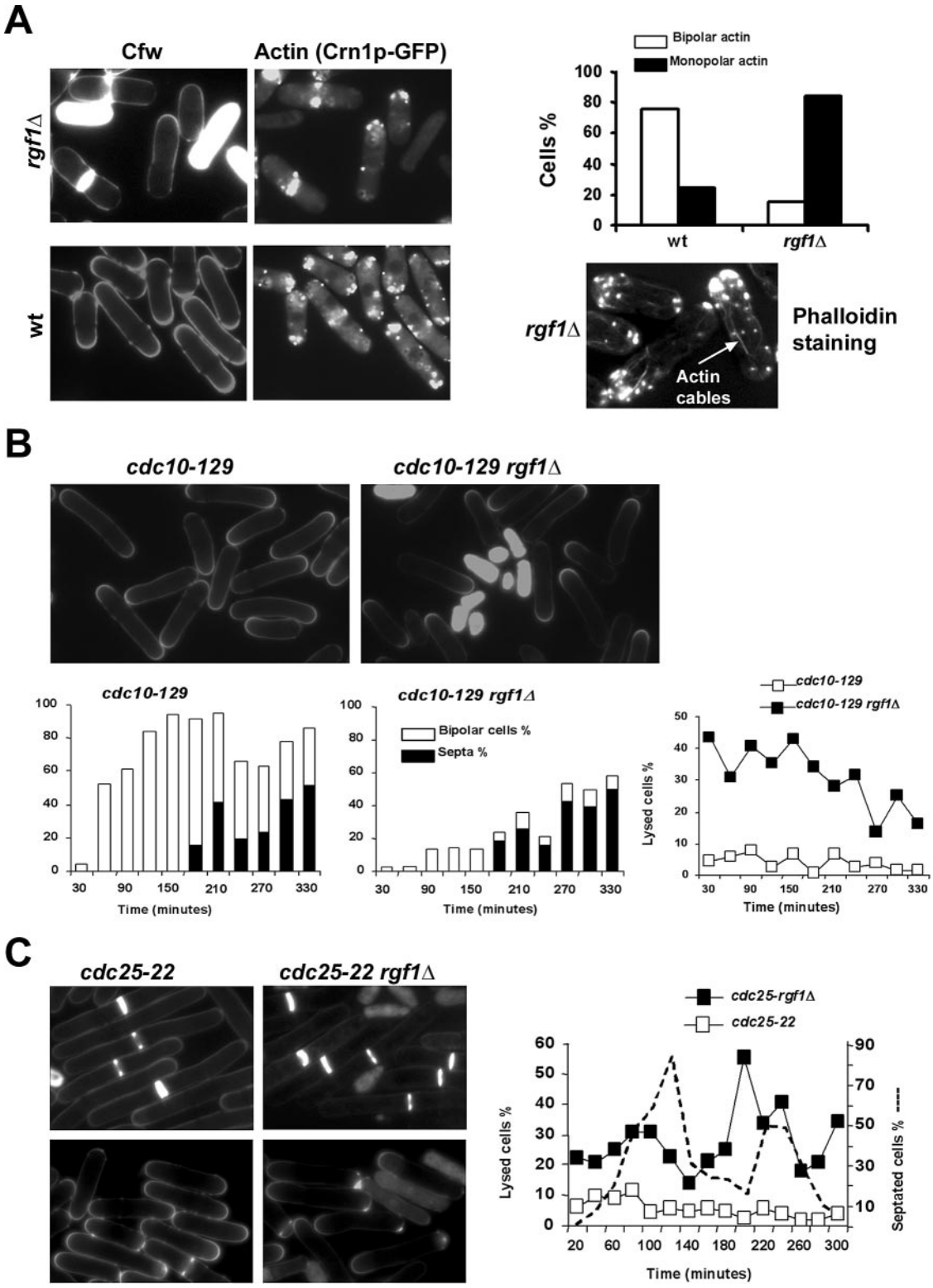

Figure 3. Rgf1p is required for bipolar growth. (A) Actin organization in *rgf1*Δ cells. Left, early-log phase cells *rgf1*$^+$*crn1*$^+$-GFP (JCR962) and *rgf1*Δ *crn1*$^+$-GFP (PG92) grown in YES liquid medium at 28°C were collected and visualized for Calcofluor (Cfw) staining and GFP (actin-associated Crn1p) fluorescence. Cfw was added at 20 μg/ml, followed by immediate examination of the cells. Note that compared with the wild type, in the *rgf1*Δ mutant the actin patches often have a more monopolar distribution. The graphic represents the percentages of monopolar and bipolar actin growth patterns in *rgf1*$^+$ (JCR962, n = 203) and *rgf1*Δ cells (PG92, n = 226) as examined by actin staining. Bottom right, *rgf1*Δ cells were fixed and stained with AlexaFluor-conjugated phalloidin to stain F-actin structures. Actin cables and patches are indicated. (B) *cdc10-129* (MS168) and *cdc10-129 rgf1*Δ (PG88) grown at 25°C to OD_{600} 0.15, shifted to 37°C for 4 h, and then grown at 25°C for 330 min. Aliquots of cells were harvested before and every 30 min after the shift to 25°C. The graphics (on the left) represents the percentage of bipolar cells (□) and septa (■) at each time point. On the right the percentage of lysed cells at each time point is represented.

RESULTS

Identification of rgf1⁺

We originally isolated *rgf1⁺* from the *S. pombe* cosmid SPCC645. In the process of cloning the gene affected in the *ehs2-1* mutation (for Echinocandin hypersensitive) we found two ORFs: *rgf1⁺* (SPCC645.07C) and *rgf3⁺* (SPCC645.06c). Both genes lay consecutive with divergent promoters and coded for proteins containing a Rho-GEF domain (the acronym *rgf* stands for RhoGEF). *rgf3⁺* is the gene affected in the *ehs2-1* mutant, whereas *rgf1⁺* partially suppresses hypersensitivity to Calcofluor (Cfw) and Echinocandin (Ech) but does not rescue lysis at 37°C in the *ehs2-1* mutant (Tajadura *et al.*, 2004).

The *rgf1⁺* gene encodes a protein of 1334 amino acids, with a predicted molecular size of ~150.1 kDa. Structural analysis of Rgf1p revealed that it contains the putative Dbl homology domain (DH; amino acid residues: aa 625-807) and a pleckstrin homology domain (PH; aa 844-973) adjacent to the DH domain characteristic of most Rho-GEFs. The DH-PH tandem is responsible for the activation of Rho-family GTPases in response to diverse extracellular stimuli (reviewed in Gulli and Peter, 2001; Rossman *et al.*, 2005). A DEP (Dishevelled, Egl-10, and Pleckstrin) domain (aa 424-497) and a CNH (Citron and NIK1-like kinase homology domain; aa 997-1293) were also found. Their function is not clear, but in most cases they act as regulatory domains involved in macromolecular interactions (http://www.genedb. org/genedb/pombe/index.jsp; Figure 1). There are seven genes that encode a putative Rho GEF domain in *S. pombe* (Coll *et al.*, 2003; Hirota *et al.*, 2003; Iwaki *et al.*, 2003; Tajadura *et al.*, 2004); among them, the closest homolog to *rgf1⁺* is *rgf2⁺*. A computer search of the deduced amino acid sequence showed that the identity percentage observed between Rgf1p and Rgf2p was ~39.4% and this rose to 63.4% upon comparing the GEF domains, whereas the identity between Rgf1p and Rgf3p (whole proteins) was 16 and 22.6% in the GEF domain.

rgf1Δ Null Cells Show Defects in Cell Integrity Similar to the Depletion of Rho1p

To characterize the relationship between Rgf1 and Rho proteins, we carried out a series of experiments to determine whether Rgf1p was acting upstream from any of the Rho proteins. First, we created a strain defective in *rgf1* by replacing the *rgf1* ORF with the *his3⁺* marker, as detailed in *Materials and Methods.* The resulting strain, *rgf1Δ*, showed a slow growth pattern at 28°C (Figure 2A), and the viability of the *rgf1Δ* cells was 55% compared with the wild-type isogenic strain. Curiously, the growth defect was less severe when *rgf1Δ* cells were grown at 37°C (unpublished data). We observed the morphology in the 25–28 to 32°C temperature range and found that regardless of the growth temperature 30–35% of the cells were lysed, whereas the rest of the cells exhibited the wild-type morphology (Figure 2B). The lysed cell phenotype of the *rgf1Δ* cells was similar to that observed in the *ehs2-1* mutant (affected in the *rgf3⁺* gene; Tajadura *et al.*, 2004) and in cells depleted for Rho1p (Arellano *et al.*, 1997). The same phenotype has also been reported in cells expressing the Rho1T20N dominant-negative mutant (Nakano *et al.*, 1997). Lysis of the *rgf1Δ* mutants cells was suppressed by the addition of 1.2 M sorbitol (Figure 2B). These phenotypes prompted us to investigate whether the mutants had a defect in cell wall architecture. We examined the sensitivity of *rgf1Δ* null mutants to different concentrations of Csp (CANCIDAS, Merck), a lipopeptide antibiotic that inhibits β(1,3)-glucan biosynthesis (Deresinski and Stevens, 2003). As shown in Figure 2C, *rgf1Δ* cells were unable to grow on plates supplemented with Csp (0.1 μg/ml), whereas the wild-type cells were able to withstand concentrations of up to 5 μg/ml (unpublished data). These results suggest that the *rgf1* null mutant cells lose their integrity, probably because of defects in cell wall biosynthesis.

The rgf1 Mutation Causes Defect in Bipolar Growth

Activation of Rho-family GTPases leads to the assembly of contractile actin-myosin filaments (Jaffe and Hall, 2005). In fission yeast, actin is organized as longitudinal F-actin cables and cortical F-actin patches at the growing ends of interphase cells, where the cell wall is newly synthesized (Marks and Hyams, 1985). To determine whether Rgf1p plays a role in any of these events, we used Crn1p-GFP (coronin), a marker for actin patches (Pelham and Chang, 2001), and Atb2p-GFP (alpha-tubulin 2) for microtubule observation (Ding *et al.*, 1998). As shown in Figure 3A, the *rgf1* mutants showed a defect in actin organization in that they organized actin patches mostly at one end of the cell only (Figure 3A, photos and graphic). This cell end corresponded to the growing end in these monopolar cells as also assessed by Calcofluor staining. Actin organization at the cell division site and F-actin cable formation was not affected in *rgf1Δ* cells (Figure 3A). We also failed to detect any significant interphase MTs defects (unpublished data).

We next investigated the behavior of *rgf1Δ* cells in the G2 phase of growth and wondered whether the lysed cell phenotype of *rgf1Δ* null mutants was due to a defect in tip elongation. To this end, we constructed the double mutant *cdc10-129 rgf1Δ* (see *Materials and Methods*) and synchronized cells in G1 by arrest at 37°C. The areas in which new cell wall deposition, and hence growth, was occurring were visualized using the fluorescent dye Calcofluor white (Cfw). Eighty minutes after being shifted to the permissive temperature 55% of *cdc10-129* cells displayed bipolar growth, whereas only 4% of *cdc10-129 rgf1Δ* cells were bipolar (Figure 3B). At 150 min after shifting, only 14% *cdc10-129 rgf1Δ* cells were bipolar. However in both strains, septation started and proceeded almost at the same time (Figure 3B, bipolar and septa plots). In this situation, the percentage of lysis in the *cdc10-129 rgf1Δ* mutant remained high (45–30%) during the first part of the time course, when bipolar growth takes place, and declined slightly in septating cells (25–15%; Figure 3B). In sum, *rgf1Δ* cells showed a defect in the activation of bipolar growth that coincided with the highest percentage of lysis.

To examine septation in *rgf1Δ* cells, we constructed the double mutant *cdc25-22 rgf1Δ* and synchronized cells in G2 by *cdc25-22* arrest at 37°C. Cells were grown at 25°C to log phase, changed to 37°C for 4 h, and then returned to 25°C. Aliquots were taken at different times to count cells with septa and lysed cells. On shifting the cells to the permissive temperature, septation was initiated at the same time in *cdc25-22* and *cdc25-22 rgf1Δ* cells. However, the second round of septation was slightly ahead in the *rgf1Δ* strain

Figure 3 (cont). Micrographs show Cfw stained *cdc10-129* and *cdc10-129 rgf1Δ* cells 60 min after the shift to 25°C. (C) *cdc25-22* (NG669) and *cdc25-22 rgf1Δ* (PG43) cells grown at 25°C to an OD_{600} 0.15, shifted to 37°C for 4 h, and then grown at 25°C for 300 min. Aliquots of cells were harvested before and every 20 min after the shift to 25°C. On the left, micrographs showing *cdc25-22* and *cdc25-22 rgf1Δ* cells 100 min (top panels) and 200 min (bottom panels) after the shift to 25°C. The graphic on the right represents the percentage of lysis of *cdc25-22*-synchronized cells (□) or *cdc25-22 rgf1Δ*-synchronized cells (■) at each time point. The septation index of *cdc25-22 rgf1Δ* cells is shown by the dashed line (– – –).

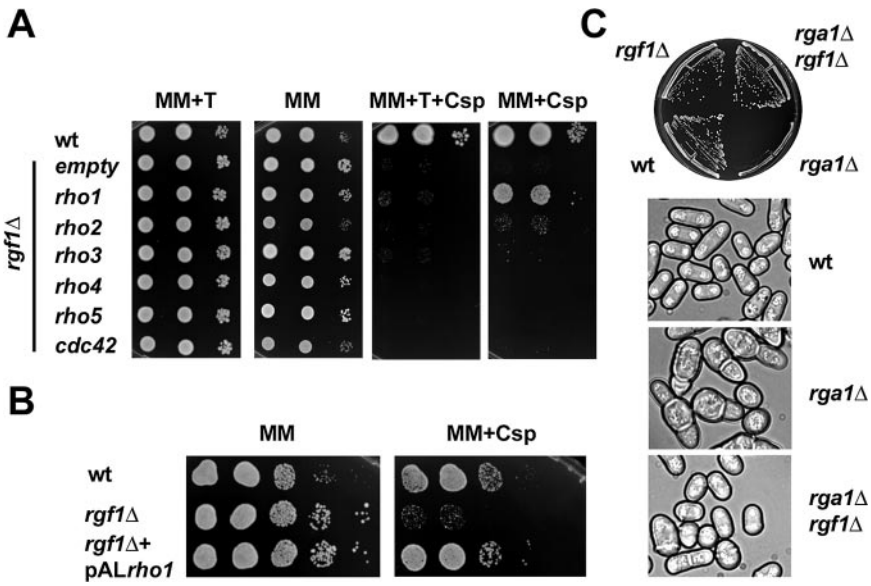

Figure 4. Rgf1p acts as a positive regulator of Rho1p. (A and B) The Caspofungin-hypersensitive growth phenotype of *rgf1*Δ mutants is suppressed by overexpression of *rho1*$^+$. HVP54 (*rgf1*$^+$) was transformed with pREP3X (empty vector), and VT14 (*rgf1*Δ) was transformed with pREP3X-*rho1* (*rho1*$^+$), pREP3X-*rho2* (*rho2*$^+$), pREP3X-*rho3* (*rho3*$^+$), pREP3X-*rho4* (*rho4*$^+$), pREP3X-*rho5* (*rho5*$^+$), pREP3X-*cdc42* (*cdc42*$^+$), and pREP3X (empty vector). Transformants were spotted onto MM, MM plus thiamine, MM plus 2 μg/ml Caspofungin (Csp), and MM plus thiamine and 2 μg/ml Csp plates as serial dilutions (4×10^4 cells in the left row and then 2×10^4 cells and 2×10^2 in each subsequent spot) and incubated at 28°C for 3 d. (B) HVP54 (*rgf1*$^+$) was transformed with pAL (empty vector) and VT14 (*rgf1*Δ) was transformed with pAL-*rho1* (*rho1*$^+$) and pAL (empty vector). Serial dilutions of the transformant cultures were spotted onto MM and MM plus 2 μg/ml Csp (from left to right 4×10^4, 2×10^4, 2×10^3, 2×10^2, 2×10) and incubated as above. (C) Deletion of *rgf1*$^+$ suppresses the growth defect in *rga1*Δ cells. Wild-type (wt) (PG75-4c), *rgf1*Δ (PG76-5a), *rga1*Δ (PG74-2b), and *rgf1rga1*Δ (PG73-1c) segregants were streaked onto YES medium and incubated at 28°C for 3 d. *rgf1rga1*Δ, but not *rga1*Δ, cells grew as wild-type cells. DIC (differential interference contrast) images of (wt) (PG75-4c), *rga1*Δ (PG74-2b), *rgf1rga1*Δ (PG73-1c)—from micromanipulation plates—grown in YES liquid medium at 28°C for 8 h are shown in the bottom panel.

(unpublished data). The appearance and number of septa were similar in both strains (Figure 3C, top panels). This result suggested that septum formation and cell separation proceeded normally in the absence of Rgf1p. However, regarding cell lysis we found a peak of broken cells in the *cdc25-22 rgf1*Δ strain just before the second round of septation, corresponding to cells in the G2 phase (Figure 3C, lower panels and graph). Thus, *rgf1*Δ cells display several phenotypes that are consistent with a role of Rgf1p in actin reorganization during activation of bipolar growth, one of the major changes in polarized growth during the *S. pombe* morphogenetic cycle.

Rgf1p Acts as a Positive Regulator of Rho1p

If *rgf1*$^+$ functions as a regulator of *rho1*$^+$, it could be expected that overexpression of *rho1*$^+$ would partially suppress the hypersensitivity to Csp as well as the lytic growth phenotype of the *rgf1* null mutant. The VT14 strain (*rgf1*Δ, *leu1-32*) was transformed with plasmids bearing *rho1*$^+$, *rho2*$^+$, *rho3*$^+$, *rho4*$^+$, *rho5*$^+$, and *cdc42*$^+$ under the control of the *nmt1* promoter or with an empty vector (pREP3X) as a control. As shown in Figure 4A, the Csp hypersensitivity of the *rgf1*Δ mutant was suppressed by *rho1*$^+$ in minimal medium without thiamine (promoter on). In minimal medium with thiamine (promoter off), no suppression was observed. None of the other genes was able to suppress the hypersensitivity of *rgf1*Δ; this being consistent with the idea that *rgf1*$^+$ could act in the same pathway as *rho1*$^+$ (Figure 4A). Overexpression of *rho2*$^+$ in wild-type cells is lethal (Hirata *et al.*, 1998), whereas overexpression of *rho1*$^+$ alone rendered the wild-type cells more sensitive to Papulacandin B (Arellano *et al.*, 1996). To avoid problems related to overexpression, we repeated the complementation experiment with the GTPases driven by the *41nmt* promoter (medium level). In this situation *rho1*$^+$ and *rho2*$^+$ constructs produced cells that exhibited wild-type morphology, however, except *for rho1*$^+$, no complementation of the hypersensitivity to Csp was found either (unpublished data). Cells that overexpressed *rho1*$^+$ from a multicopy plasmid, under the control of its own promoter behaved as wild-type cells regarding growth either with or without Csp (unpublished data). Interestingly, this construct, fully suppressed the *rgf1*Δ mutant hypersensitivity to Csp (Figure 4B) and cell lysis.

To gain further evidence that Rgf1p was a GEF for Rho1p, we tested whether an *rgf1* null mutation was able to counteract a mutation in Rga1p, a protein with GAP activity toward Rho1p and hence a negative regulator (Nakano *et al.*, 2001). Lack of Rga1p produces small colonies and the cells show a swollen, multiseptated or branched shape; a phenotype similar to that seen in cells in which Rho1p is excessively activated (Figure 4C; Nakano *et al.*, 2001). We replaced the *rgf1*$^+$ gene with the *his3*$^+$ marker in a diploid strain, *rga1*Δ/*rga1*$^+$, and the *rgf1*Δ, *rga1*Δ, *rgf1rga1*Δ segregants from 16 tetrads were analyzed. We found that the *rgf1*Δ*rga1*Δ cells formed regularly sized colonies, like *rgf1*Δ cells (unpublished data). When *rgf1*Δ, *rga1*Δ, *rgf1*Δ*rga1*Δ strains (respectively) were streaked out on rich medium (YES) at 28°C, the *rga1*Δ cells were severely impaired for growth, whereas *rgf1*Δ*rga1*Δ exhibited a better growth pattern and resembled *rgf1*Δ cells. The rounded and branched shape seen in the *rga1*Δ mutant cells returned to the wild-type morphology in the double mutant *rgf1*Δ*rga1*Δ cells (Figure 4C). Thus, *rgf1*$^+$ and *rga1*$^+$ indeed appear to antagonize each other, presumably acting on the same Rho-like GTPase.

Rgf1 Associates with Rho1p in S. pombe Cells and Promotes the GDP-GTP Exchange

To examine whether there was a direct interaction between Rgf1p and Rho1p in *S. pombe* cells, we performed coprecipitation experiments. We coexpressed HA-epitope–tagged Rgf1 protein (Rgf1-HA) together with either GST-Rho1 or GST in *S. pombe* cells. Cells were lysed, and the supernatant fractions of the lysates were incubated with glutathione-Sepharose beads to isolate GST complexes, which were analyzed by immunoblotting. As shown in Figure 5A,

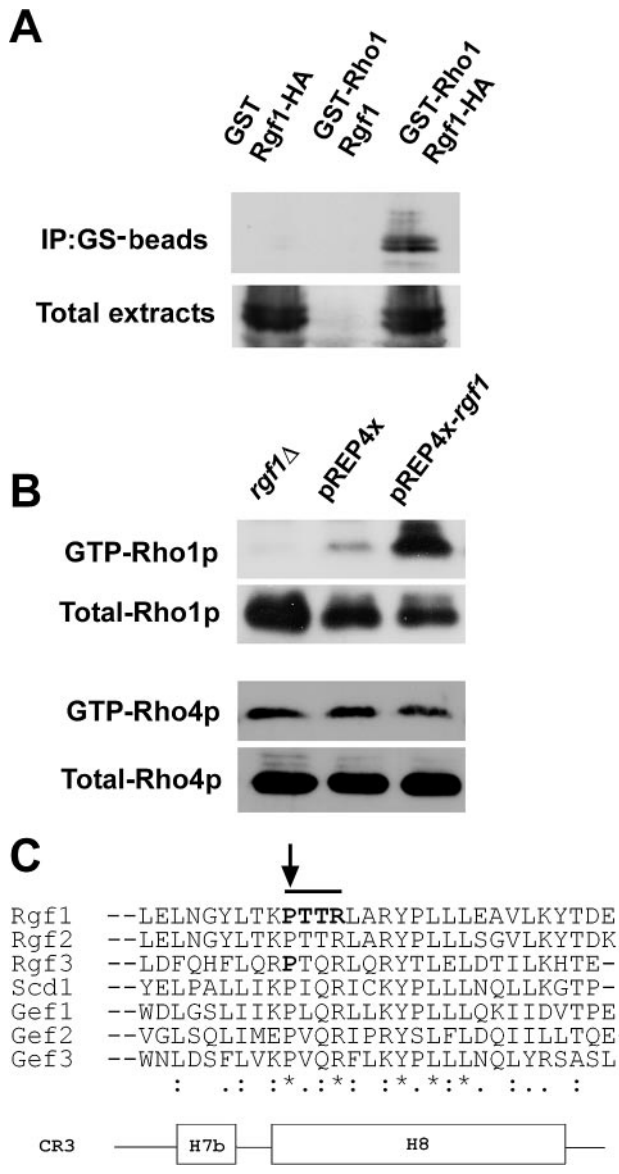

Figure 5. Rgf1p is a specific Rho1-GEF. (A) Coprecipitation of Rgf1p and Rho1p. Cell extracts from cells expressing, GST and Rgf1p-HA; GST-Rho1p and Rgf1p, and GST-Rho1p and Rgf1p-HA were precipitated with glutathione beads and blotted against 12CA5 monoclonal anti-HA antibody (top). Western blot with anti-HA antibody was performed on total extracts to visualize total Rgf1p-HA levels (bottom). (B) In vivo, the Rgf1p level modulates the amount of GTP-bound Rho1p. Wild-type (YS64) cells expressing pREP4X or pREP4X-*rgf1*, and *rgf1*Δ (VT14) mutant cells were transformed with either pREP3X-HA-*rho1* or pREP3X-HA-*rho4*. GTP-Rho1p or GTP-Rho2p were pulled down from the cell extracts with GST-C21RBD and blotted against 12CA5, anti-HA mAb. Total HA-Rho1p and HA-Rho4p was visualized by Western blot. (C) Alignment of predicted amino acid sequence at the CR3 region of Rgf1p with the corresponding region of proteins with a Rho-GEF domain found in *S. pombe*. Multiple sequence alignments were performed using the ClustalW program. The amino acids deleted in the *rgf1-PTTR*Δ mutant are marked with "black caps" over the predicted amino-acid sequence of Rgf1p. The proline (P) mutated in the *rgf3* mutant (*ehs2-1*) is also highlighted and signaled by an arrow. Asterisks indicate identical amino acids among all identified gene products. (.) and (:) indicate well- and highly-conserved amino acids, respectively.

Rgf1-HA was found to be associated with GST-Rho1, but not with GST.

To further investigate the possible role of Rgf1p as a Rho1p activator, we analyzed the in vivo amount of GTP-bound Rho1p in cells with different amounts of Rgf1p. *rgf1*Δ mutant cells carrying the control plasmid pREP4X and wild-type cells carrying either pREP4X or pREP4X-*rgf1*$^+$ were transformed with pREP3X-*HA-rho1*$^+$. After induction of the *nmt1* promoter for 18 h, the amount of Rho1p bound to GTP was analyzed by precipitation with GST-C21RBD, the rhotekin-binding domain (which had previously been obtained and purified from bacteria) and blotting with anti-HA antibody (Figure 5B). Western blots of whole extracts (25 μg protein) showed that the total amount of Rho1p was similar in all three strains with different amounts of Rgf1p (Figure 5B). The amount of active Rho1p increased considerably in the strain overexpressing Rgf1p compared with the wild-type strain. Moreover, only a minor amount of GTP-Rho1p was detected in the strain lacking Rgf1p. As a control, we also analyzed the amount of GTP-bound Rho4p in *rgf1*Δ, wild-type, and cells overexpressing *rgf1*$^+$ (Figure 5B, bottom panel). These cells were transformed with the plasmid pREP3X-HA-*rho4*$^+$ and GTP-bound Rho4p was pulled down from the extract by binding to GST-C12RBD. No changes in the level of Rho4p bound to GTP were observed among the three strains (Figure 5B). These results provide evidence that Rgf1p interacts with Rho1p and acts as a specific Rho1p activator in *S. pombe*. To examine whether the GEF domain was essential for Rgf1p function, we created a deletion mutant in the RhoGEF domain of Rgf1p (*rgf1-PTTR*Δ; Figure 5C). The DH domain contains three conserved blocks of sequences that have previously been referred to as conserved regions 1–3, or CR1–3. These three conserved regions form three long helices, H1a, H2b, and H8, which pack together to form the core of the DH domain. The four amino acids that were deleted in the *rgf1-PTTR*Δ mutant (proline-threonine-threonine-arginine, PTTR) have been predicted to be located on helix H8 (CR3), which is the most highly conserved region of the DH domain and where many mutations that decrease nucleotide exchange activity map (Liu *et al.*, 1998; Soisson *et al.*, 1998). Moreover, a single change from a proline to a serine in that conserved region of Rgf3p is responsible for the thermosensitive lytic phenotype in the *ehs2-1* mutant (Tajadura *et al.*, 2004). We found that the *rgf1-PTTR*Δ mutant integrated in a single copy in *rgf1*Δ strain maintained the lytic and the Csp-hypersensitive phenotype of the *rgf1*Δ null mutants, thus supporting the hypothesis that Rgf1p acts as a GEF.

rgf1$^+$ *Overexpression Causes Aberrant Morphology and Increases β(1,3)-glucan Synthase Activity*

It has previously been reported that overexpression of *rho1*$^+$ or constitutively active *rho1* mutants from the strong *nmt1* promoter causes an aberrant morphology in *S. pombe* cells (Arellano *et al.*, 1996; Nakano *et al.*, 1997). If *rgf1*$^+$ functions as a positive regulator of Rho1p, overexpression of *rgf1*$^+$ would be expected to produce phenotypes similar to that of Rho1-overexpressing cells. The *rgf1*$^+$ gene was cloned under the thiamine-repressible *nmt1* promoter in the pREP3X vector. When thiamine was eliminated to enhance *rgf1*$^+$ expression, the cells were unable to grow on plates (unpublished data). After 18 h of induction, cells were larger than the wild-type, round, or misshapen, with abnormal septa. These cells also showed a general increase in Cfw fluorescence, some containing aberrant depositions of Cfw-stainable material (see cells marked with an arrow and enlarged cells in Figure 6A).

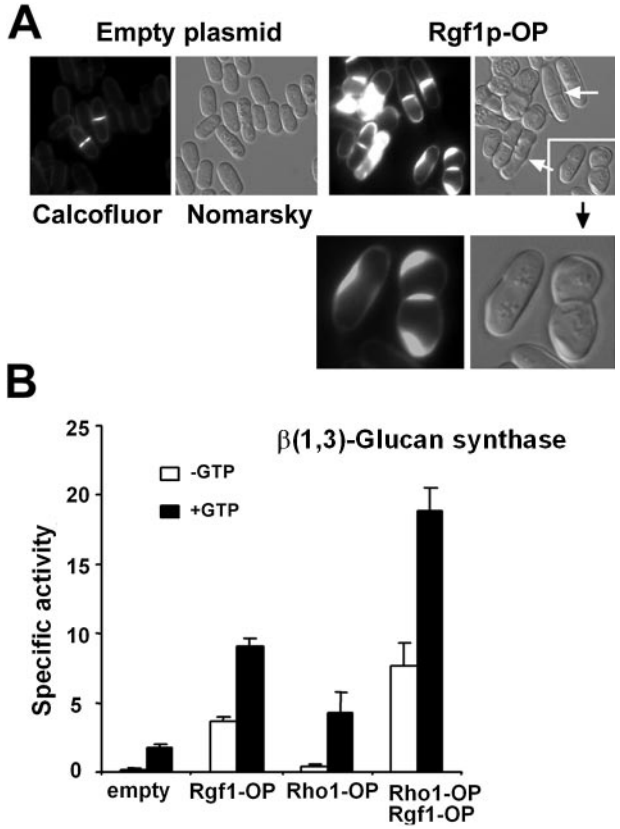

Figure 6. Phenotypes of Rgf1p overexpression (OP). (A) Overexpression of *rgf1*$^+$ causes cell growth arrest and an abnormal accumulation of cell wall material. DIC and Calcofluor-stained UV micrographs of wild-type cells transformed with pREP3X (empty plasmid) or pREP3X-*rgf1* (Rgf1-OP) grown without thiamine for 18 h. (B) In vitro glucan synthase (GS) activity assayed with the membrane fraction of wild-type cells (HVP54) transformed with pREP3X (empty plasmid), pREP3X-*rgf1* (Rgf1-OP), pREP3X-*rho1* (Rho1-OP), or both pREP4X-*rgf1* and pREP3X-*rho1* (Rgf1-OP and Rho1-OP). Extracts were prepared from cells grown in MM without thiamine at 32°C for 18 h. Specific activity is expressed as milliunits mg^{-1} protein. Values are means of at least three independent experiments with duplicated samples, and error bars represent SDs.

As expected, GS activity increased during *rgf1*$^+$ overexpression. This activity was fourfold higher than that observed in the wild-type strain (Figure 6B). To corroborate these results, we also studied the activity in cells that overexpressed *rho1*$^+$ and *rgf1*$^+$ at the same time (transformed with pREP3X-*rho1* and pREP4X-*rgf1* plasmid). As described previously, cells overexpressing *rho1*$^+$ showed an increase in GS activity (Figure 6B; Arellano *et al.*, 1996). This increase was considerably (10-fold) higher in cells that overexpressed *rgf1*$^+$ at the same time (Figure 6B). These results clearly indicate that Rgf1p is involved in the regulation of β(1,3)-glucan biosynthesis.

Genetic Evidence that Rgf1p Interacts Functionally with Bgs4p and Pck1p

It is known that Rho1p functions by activating β-glucan biosynthesis, but the issues of which of the GS catalytic subunits it activates, remain unclear. In a previous work, we reported that a mutation in *rgf3*$^+$ (*ehs2-1* mutation) was suppressed by *bgs3*$^+$, one of the putative β(1,3)-GS subunits. Multiple copies of *bgs3*$^+$ complemented the hypersensitivity to Ech and Cfw but not the temperature-sensitive phenotype (Martin *et al.*, 2003). To define a possible relationship between Rgf1p and known Rho1p effectors, we first tested whether overexpression of any of the β-GS subunits could suppress the hypersensitive phenotype of the *rgf1*Δ mutants. The *rgf1* strain VT14 was transformed with the high-copy number plasmids pAL-*bgs1*$^+$, pAL-*bgs2*$^+$, pAL-*bgs3*$^+$, and pAL-*bgs4*$^+$, and transformants were monitored for growth in Csp. As shown in Figure 7A, only a moderate expression of *bgs4*$^+$ restored growth of an *rgf1*Δ mutant in the presence of the antifungal agent. We also examined the consequences of overexpressing *rgf1*$^+$ in *cwg1-1* cells, which hold a nonlethal thermosensitive mutation in the essential *bgs4*$^+$ gene (Cortes *et al.*, 2005). When the *cwg1-1* strain was transformed with the *rgf1*$^+$ gene driven by the *nmt1* promoter, neither the pREP3X-*rgf1* with thiamine (promoter off) nor the same without thiamine (promoter on) suppressed lysis at 37°C of *cwg1-1* cells (unpublished data). In addition, *rgf1*Δ *cwg1-1* cells were phenotypically similar to *cwg1-1* (*bgs4*) cells at 37°C (Figure 7B). This finding, combined with the above observations, suggests that Rgf1p specifically activates the Rho1p-Bgs4p GS complex.

Another target of Rho1p in *S. pombe* are the PKC homologues Pck1p and Pck2p; Both genes—*pck1*$^+$ and *pck2*$^+$—share overlapping roles in cell viability and partially complement each other (Toda *et al.*, 1993); Pck2p also plays a role in the regulation of the β(1,3)-GS membrane component (Arellano *et al.*, 1999b). Because overexpression of Rho1p suppresses hypersensitivity to Csp in *rgf1*Δ mutants, we asked ourselves whether the overexpression of either Pck1p or Pck2p might function in a similar way. The *rgf1*Δ strain VT14 was transformed with the high-copy number plasmids pDB248-*pck1*$^+$and pDB248-*pck2*$^+$ (Toda *et al.*, 1993), and transformants were monitored for growth on Csp. As shown in Figure 7C, only a moderate expression of *pck1*$^+$ restored growth of an *rgf1*Δ mutant in the presence of the antifungal agent.

Rgf1p Localizes to One or Both Poles during Cell Growth and to the Contractile Ring and Septum during Cytokinesis

To determine the subcellular localization of Rgf1p, the coding sequence of the green fluorescence protein (GFP) was fused in-frame before the *rgf1*$^+$ stop codon. The GFP-*rgf1*$^+$ *rgf1*Δ strain (GFP at amino acid 1334, integrated in single copy, with its own promoter and in the absence of original *rgf1*$^+$ gene) completely restored the wild-type phenotype to *rgf1*Δ mutant cells. The cells were visualized using GFP fluorescence in order to detect Rgf1p and by Cfw staining. Rgf1p was found to localize to the growing ends and septum along the mitotic cycle, overlapping with Cfw staining (Figure 8A). When cell growth began, Rgf1p accumulated at the old growing end. During bipolar growth, Rgf1p also localized to the opposite pole. Finally, the GFP disappeared from both poles and localized only to the middle of the cell, concentrating as two faint dots on either side of the emerging septum. The GFP then moved to the inner border of the growing septum, forming a ring that moved centripetally with the edge of the growing septum (Figure 8B). After the septum wall had been completed, the GFP appeared in two separate bands (unpublished data). During cell division, Rgf1p remained on both sides of the septum until the two daughter cells were ready to separate or had already done so. To confirm these observations, confocal microscopy was used. The results of the 3-D reconstruction of the green fluorescence indicated that during septum formation Rgf1p-GFP was localized to a platelike structure; fluorescence was

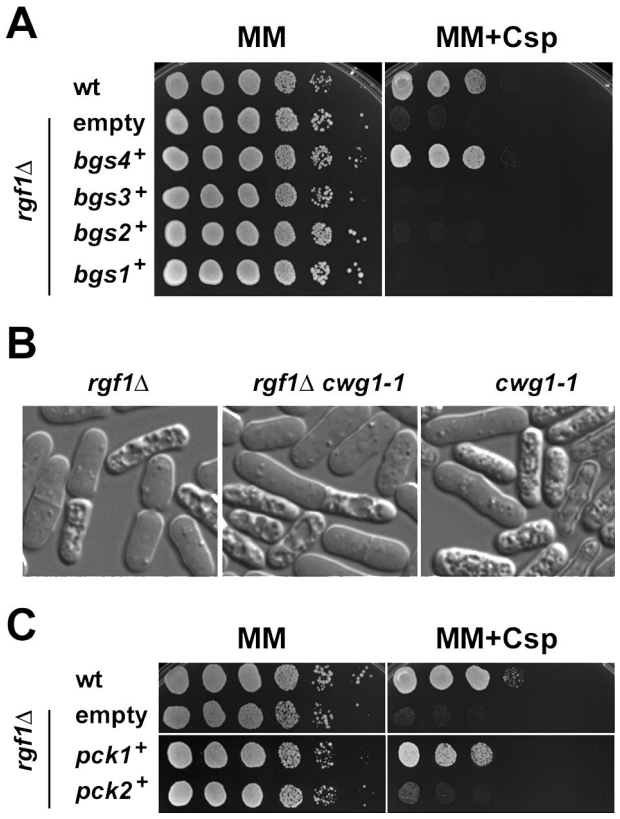

Figure 7. The Caspofungin-hypersensitive growth phenotype of *rgf1*Δ mutants is suppressed by overexpression of *bgs4*$^+$ and *pck1*$^+$. (A) HVP54 (*rgf1*$^+$) was transformed with pAL (empty vector) and VT14 (*rgf1*Δ) was transformed with pAL (empty vector), pAL-*bgs4* (*bgs4*$^+$), pAL-*bgs3* (*bgs3*$^+$), pAL-*bgs2* (*bgs2*$^+$), and pAL-*bgs1* (*bgs1*$^+$). Transformants were spotted onto MM and MM plus 2 μg/ml Csp plates as serial dilutions (8×10^4 cells in the left row and then 4×10^4, 2×10^4, 2×10^3, 2×10^2, and 2×10^1 in each subsequent spot) and incubated at 28°C for 3 d. (B) PG76 (*rgf1*Δ), JCR132 (*cwg1-1*), and PG82 (*rgf1*Δ *cwg1-1*) cells derived from a cross between strains PG76 (*rgf1*Δ) and JCR132 (*cwg1-1*) were grown to log phase in rich medium at 28°C, shifted for 4 h to 37°C, and then visualized under differential interference contrast (DIC) microscopy. The relevant genotype of each strain is indicated at top of each panel. (C) HVP54 (*rgf1*$^+$) was transformed with pDB248 (empty vector) and VT14 (*rgf1*Δ) was transformed with pDB248 (empty vector), pDB248-*pck1* (*pck1*$^+$), and pDB248-*pck2* (*pck2*$^+$). Transformants were spotted onto MM and MM plus 2 μg/ml Casp plates and processed as in A.

ring-shaped in the first stages, and as the ring was closing the fluorescence remained behind the edge and ended up distributed as a division plate (Figure 8C).

Rgf1p localized to growing areas (septum and poles) and played an important function during bipolar growth; Rgf3p localizes and functions specifically during cytokinesis (Tajadura *et al.*, 2004). We therefore investigated whether the role of Rgf1p in the regulation of Rho1p was overlapping that of Rgf3p. Previous work had shown that moderate expression of *rgf1*$^+$ did not suppress lysis at 37°C of the *rgf3* mutant (*ehs2-1*; Tajadura *et al.*, 2004). We wondered if the opposite was also true; whether overexpression of *rgf3*$^+$ was able to suppress the hypersensitive phenotype or the lysis of the *rgf1*Δ strain. *rgf3*$^+$, driven either by its own promoter or by the *nmt1* promoter, was not able to suppress the hypersensitivity in the presence of Csp nor the lysis of *rgf1*Δ cells. Moreover, disruption of *rgf1*$^+$ in an *rgf3* mutant (*ehs2-1*) produced viable cells at 28°C but not at 37°C, the temperature at which both mutants were able to grow on plates (unpublished data). These result support the hypothesis that Rgf1p and Rgf3p are not functionally interchangeable. Previous studies (Iwaki *et al.*, 2003; Tajadura *et al.*, 2004) and our own results suggest that both Rgf3p and Rgf1p are GEFs of Rho1p. The experiments reported here indicate that Rgf1p activates a Rho1p pathway (Rho1p-Bgs4p) other than that activated by Rgf3p.

DISCUSSION

Guanine nucleotide exchange factors (GEFs) are directly responsible for the activation of Rho-family GTPases in response to diverse stimuli and ultimately regulate many cellular responses such as proliferation, differentiation, and movement (Rossman *et al.*, 2005). Seven Rho-GEFs belonging to the Dbl family of proteins have been identified in *S. pombe* (Iwaki *et al.*, 2003). Here we studied the Rho-GEF, designated Rgf1, which like other Rho-GEFs contains the DH-PH tandem motifs required to activate Rho proteins (Schmidt and Hall, 2002).

Here we have shown that Rgf1p is likely to be a GEF for Rho1p. *rgf1*Δ cells are defective in cell integrity and lyse with a phenotype similar to cells devoid of Rho1 or Pck1/2 activity. Moreover, mutants lacking *rgf1* display a defect in actin organization and in β-glucan biosynthesis. The fact that both processes are controlled by Rho1p suggests that the main function of Rgf1p would be to regulate this GTPase. Consistent with this idea, the hypersensitivity to Csp and the lytic phenotype were suppressed by overexpression of *rho1*$^+$ but not other *rho* genes. Additionally, we provide genetic and biochemical evidence to support the view that Rgf1p interacts functionally with and acts as a positive regulator of Rho1p: 1) Deletion of *rgf1*$^+$ suppresses the slow growth defect of a null mutant in the *rga1*$^+$ gene, encoding a GTPase-activating protein for Rho1 (Nakano *et al.*, 2001). This finding suggests that Rgf1 may play a role antagonistic to that of Rga1p GAP. 2) Rgf1p specifically coprecipitated with Rho1p, and the level of Rgf1p modulated the level of GTP-Rho1p in vivo. 3) Overexpression of *rgf1*$^+$ was lethal and caused a phenotype similar to that of the constitutively active allele *Rho1G15V* in wild-type *S. pombe* cells, whereas it was not deleterious when overexpressed in a GTPase-deficient Rho1p strain (Rho1F85I; S. Rincón and P. Pérez, unpublished data). Furthermore, we found that the GEF domain of Rgf1p was essential for its function; a deletion mutation in a highly conserved region of the Rgf1p-DH-domain produced a lack of function phenotype. We also found that a functional GEF domain was not necessary for its localization, because the mutated protein tagged with GFP localized correctly (unpublished data).

In *S. pombe*, Rho1p signaling is required to maintain cell integrity, regulating the biosynthesis of β(1,3)-glucan and the cell wall in general, and it is also required for actin polymerization. The experiments reported in this study indicate that *rgf1*$^+$ is involved in the regulation of cell wall biosynthesis. *rgf1*Δ mutant cells were unable to grow at 50-fold lower concentrations of the antifungal drug Csp than wild-type cells and showed a lytic phenotype that could be rescued by the presence of 1.2 M sorbitol. Cells that overexpressed *rgf1*$^+$ showed aberrant depositions of Cfw-stainable material, accompanied by a GS activity that was 5-fold that of wild-type cells. Furthermore, cells overexpressing *rgf1*$^+$ together with *rho1*$^+$ showed a huge increase in GS activity (approximately 7- to 10-fold) compared with the wild-type level. Even without GTP added to the reaction, the GS

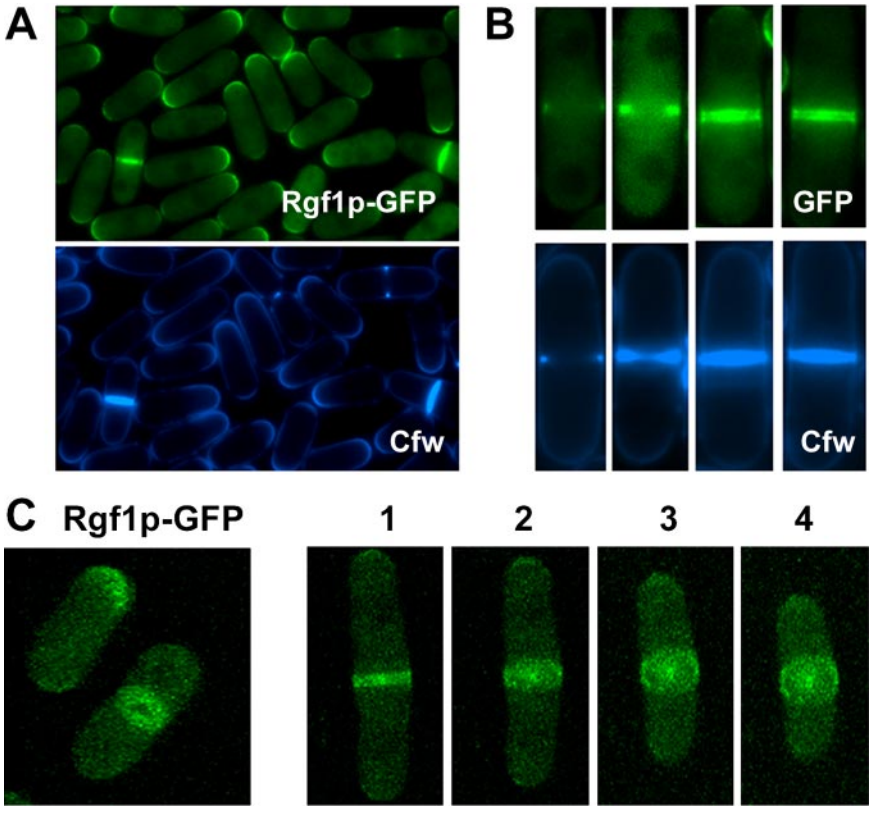

Figure 8. Rgf1p localizes to the growing regions: one or both poles, the medial ring, and the septum. (A) Rgf1p-GFP localization at different stages of the cell cycle. Early log phase cells containing the *rgf1*$^+$*-GFP* fusion allele were visualized for GFP fluorescence and Cfw staining. Cfw was added at 20 μg/ml, followed by immediate examination of the cells (bottom panel). (B) Magnification of Rgf1p-GFP localization to the medial ring and along the plasma membrane during septum formation. The cells shown were chosen from among a population of >50 dividing cells. (C) Three-dimensional reconstruction of Rgf1p localization. Cells containing the *rgf1*$^+$*-GFP* fusion allele observed under a confocal microscope and z-sections of 0.3 mm were taken. The image was reconstructed using LMS510 software.

activity of cells that overproduced *rgf1*$^+$ was 20 times higher than in the wild type, indicating that an excess of Rgf1p had raised the intracellular pool of GTP-bound Rho1p (already activated). Furthermore, our results suggest that Rgf1p would activate the β-GS complex containing the catalytic subunit Bgs4p. Rgf1p, Rho1p, and Bgs4p localize to growth areas, the septum and the poles (Arellano *et al.*, 1997; Cortes *et al.*, 2005). Individual mutants (in *rgf1*$^+$ and *bgs4*$^+$) showed similar cell wall–related phenotypes (lysis and hypersensitivity to antifungal drugs), and the double mutant *rgf1*Δ *cwg1-1* was very similar to *bgs4* (*cwg1-1*) single mutant. Moreover, overexpression of *bgs4*$^+$ suppressed the *rgf1*Δ hypersensitive phenotype.

The interaction observed between Rgf1p and Pck1p is more intriguing because the role of Pck1p in cell wall integrity remains to be established. The patterns of cell wall regulation by Pck1p and Pck2p seem to be different. *pck1*Δ, but not *pck2*Δ, cells are hypersensitive to Ech and additional copies of Pck2p cannot suppress this phenotype (Arellano *et al.*, 1999b), suggesting that in the absence of Pck1p the genes specifically involved in protection against antifungal drugs cannot be turned on. The fact that multiple copies of *pck1*$^+$ (with its own promoter) are able to suppress Csp hypersensitivity in *rgf1*Δ mutants is in agreement with the notion of Pck1p kinase being an effector of Rho1p and suggests that Pck1p would be necessary for the activation of genes (probably *bgs4*$^+$ or other GS) in response to signaling after cell wall damage. In fact, mild overexpression of either *bgs4*$^+$ (our unpublished observations), *bgs1*$^+$ or *bgs2*$^+$ (Arellano *et al.*, 1999b) was able to suppress the hypersensitive phenotype of *pck1*Δ mutants.

Activation of Rho family GTPases leads to the assembly of contractile actin:myosin filaments (Jaffe and Hall, 2005). In *S. pombe*, actin patch disassembly is one of the effects of Rho1p depletion. Interestingly, *rgf1*Δ cells showed a defect in the actin reorganization required for the transition from monopolar to bipolar growth. Among the genes required for NETO, *tea1*$^+$ plays a critical function; the most penetrant phenotype of *tea1*Δ mutants is their failure to initiate growth at the new cell tip, such that these cells only grow in a monopolar manner (Verde *et al.*, 1995; Mata and Nurse, 1997). Tea1p has been found to form a large protein complex; during NETO, the tea1p-complex at the cortex interacts with formins (and probably other polarity factors), triggering actin cable assembly and polarized cell growth (Martin *et al.*, 2005). In a *tea1*Δ mutant, Rgf1p was not maintained at one of the new cell ends, and the cells did not grow at that end (unpublished data). Rgf1p may function downstream from Tea1p, because Tea1p is required to recruit Rgf1p to a new end. The identification of proteins that directly interact with Rgf1p will be necessary to understand how Rho1p participates in the transition in which monopolar cells initiate bipolar growth.

Mutants defective in monopolar growth, *tea1*Δ, *tea4*Δ, and *bud6*Δ, grew at wild-type rates. However, a novel aspect of the *rgf1*Δ mutants is that their failure to initiate bipolar growth was accompanied by cell lysis. In a *cdc10-129 rgf1*Δ mutant, which at the restrictive temperature arrested in G1, before the activation of bipolar growth, 45% of the cells lysed 30 min after release from the restrictive temperature, whereas in a *cdc25-22 rgf1*Δ mutant, which at high temperature arrested in G2 with both ends growing, the highest percentage of lysis (55%) after release was seen after the first round of septation, coinciding in time with bipolar growth activation. Our current model is that activation of Rho1p, and in consequence β-GS activation, during bipolar growth is not achieved properly in *rgf1*Δ mutants, producing cell wall weakness. To our knowledge, *rgf1*$^+$ is the first gene that

has been implicated in cell wall biogenesis and NETO and might well provide a link between these two processes.

Rgf1p is the second exchange factor identified for Rho1p. Why does Rho1p have multiple GEFs? A similar situation has been described for mammalian cells, where the number of Rho-GEFs (~69 members) exceeds the number of Rho-type GTPases (so far 22 members; Rossman *et al.*, 2005). An attractive hypothesis is that the GEF could determine the downstream signaling specificity of Rho GTPases. This has been suggested for Ras signaling in fission yeast, where two GEFs, Ste6p and Efc25p, differentially regulate two Ras pathways (Papadaki *et al.*, 2002). In agreement with such a hypothesis, we propose that Rgf1p would specifically activate the Rho1-GS complex during the transition from monopolar to bipolar growth, whereas Rgf3p, the former Rho1-GEF, would accumulate at the contractile ring, probably activating the Rho functions that coordinate cell-wall biosynthesis to maintain cell integrity during septation (Tajadura *et al.*, 2004). Moreover, our results suggest that Rho1-GEFs, Rgf1p and Rgf3p, are not functionally interchangeable; each single *rgf1*Δ and *ehs2-1* mutant was able to grow on plates at 37°C, whereas the double *rgf1*Δ *ehs2-1* mutant was not.

In conclusion, here we provide evidence that Rgf1p is a new Rho1-GEF that participates in the regulation of bipolar growth and we propose that Rgf1p may coordinate a growth polarity transition with cell wall biosynthesis to prevent losses of cell integrity and allow cell expansion.

ACKNOWLEDGMENTS

We thank P. Perez, P. Coll, H. Valdivieso, A. Duran, and J. C. Ribas for plasmids, strains, and help along this work. C. Roncero is acknowledged for his very helpful comments. We also thank C. Castro for help with confocal microscopy. P.G. and I G. were supported by a fellowship from the Junta de Castilla y León and V. Tajadura acknowledges support from a fellowship granted by the Ministerio de Educación y Ciencia, Spain. Text was revised by N. Skinner. This work was supported by Grant BIO2001–1663 from the Comisión Interministerial de Ciencia y Tecnología, Spain and CSI02C05 from the Junta de Castilla y León.

REFERENCES

Arellano, M., Duran, A., and Perez, P. (1997). Localization of the *Schizosaccharomyces pombe* Rho1 GTPase and its involvement in the organization of the actin cytoskeleton. J. Cell Sci. *110*, 2547–2555.

Arellano, M., Durán, A., and Pérez, P. (1996). Rho1 GTPase activates the (1–3)b-D-glucan synthase and is involved in *Schizosaccharomyces pombe* morphogenesis. EMBO J. *15*, 4584–4591.

Arellano, M., Valdivieso, M. H., Calonge, T. M., Coll, P. M., Durán, A., and Pérez, P. (1999b). *Schizosaccharomyces pombe* PKC homologues, pck1p and pck2p, are targets of rho1p and rho2p and differentially regulate cell integrity. J. Cell Sci. *112*, 3569–3578.

Bähler, J., Wu, J.-Q., Longtine, M. S., Shah, N. G., McKenzie, A., III, Steever, A. B., Wach, A., Philippsen, P., and Pringle, J. R. (1998). Heterologous modules for efficient and versatile PCR-based gene targeting in *Schizosaccharomyces pombe.* Yeast *14*, 943–951.

Calonge, T. M., Arellano, M., Coll, P. M., and Perez, P. (2003). Rga5p is a specific Rho1p GTPase-activating protein that regulates cell integrity in *Schizosaccharomyces pombe.* Mol. Microbiol. *47*, 507–518.

Chang, F., and Verde, F. (2004). Control of cell polarity and morphogenesis in fission yeast. In: The Molecular Biology of *Schizosaccharomyces pombe.* Genetics, Genomics and Beyond., ed. R. Egel:, New York: Springer, 255–268.

Coll, P. M., Trillo, Y., Ametzazurra, A., and Perez, P. (2003). Gef1p, a new guanine nucleotide exchange factor for Cdc42p, regulates polarity in *Schizosaccharomyces pombe.* Mol. Biol. Cell *14*, 313–323.

Cortes, J. C., Carnero, E., Ishiguro, J., Sanchez, Y., Duran, A., and Ribas, J. C. (2005). The novel (1,3)b-D-glucan synthase catalytic subunit Bgs4p from fission yeast is essential during both cytokinesis and polarized growth. J. Cell Sci. *118*, 157–174.

Cortes, J. C., Ishiguro, J., Duran, A., and Ribas, J. C. (2002). Localization of the (1,3)beta-D-glucan synthase catalytic subunit homologue Bgs1p/Cps1p from fission yeast suggests that it is involved in septation, polarized growth, mating, spore wall formation and spore germination. J. Cell Sci. *115*, 4081–4096.

Craven, R. A., Griffiths, D. J., Sheldrick, K. S., Randall, R. E., Hagan, I. M., and Carr, A. M. (1998). Vectors for the expression of tagged proteins in *Schizosaccharomyces pombe.* Gene *221*, 59–68.

Deresinski, S. C., and Stevens, D. A. (2003). Caspofungin. Clin. Infect. Dis. *36*, 1445–1457.

Ding, D. Q., Chikashige, Y., Haraguchi, T., and Hiraoka, Y. (1998). Oscillatory nuclear movement in fission yeast meiotic prophase is driven by astral microtubules, as revealed by continuous observation of chromosomes and microtubules in living cells. J. Cell Sci. *111*, 701–712.

Duran, A., and Perez, P. (2004). Cell wall synthesis. In: The Molecular Biology of *Schizosaccharomyces pombe.* Genetics, Genomics and Beyond, ed. R. Ege, New York: Springer, 269–276.

Forsburg, S. L., and Sherman, D. A. (1997). General purpose tagging vectors for fission yeast. Gene *191*, 191–195.

Gachet, Y., Mulvihill, D. P., and Hyams, J. S. (2004). The fission yeast actomyosin cytoskeleton. In: The Molecular Biology of *Schizosaccharomyces pombe.* Genetics, Genomics and Beyond., ed. R. Egel, New York: Springer, 225–242.

Gulli, M. P., and Peter, M. (2001). Temporal and spatial regulation of Rho-type guanine-nucleotide exchange factors: the yeast perspective. Genes Dev. *4*, 365–379.

Hayles, J. A., and Nurse, P. (2001). A journey into space. Nat. Rev. Mol. Cell Biol. *2*, 647–656.

Hirata, D., Nakano, K., Fukui, M., Takenaka, H., Miyakawa, T., and Mabuchi, I. (1998). Genes that cause aberrant cell morphology by overexpression in fission yeast: a role for a small GTP-binding protein Rho2 in cell moephogenesis. J. Cell Sci. *111*, 149–159.

Hirota, K., Tanaka, K., Ohta, K., and Yamamoto, M. (2003). Gef1p and Scd1p, the two GDP-GTP exchange factors for Cdc42p, form a ring structure that shrinks during cytokinesis in *Schizosaccharomyces pombe.* Mol. Biol. Cell *14*, 3617–3627.

Iwaki, N., Karatsu, K., and Miyamoto, M. (2003). Role of guanine nucleotide exchange factors for Rho family GTPases in the regulation of cell morphology and actin cytoskeleton in fission yeast. Biochem. Biophys. Res. Commun. *312*, 414–420.

Jaffe, A. B., and Hall, A. (2005). Rho GTPases: biochemistry and biology. Annu. Rev. Cell Dev. Biol. *21*, 247–269.

Kobori, H., Yamaka, N., Taki, A., and Osumi, M. (1989). Actin is associated with the formation of the cell wall in reverting protoplasts of the fission yeast *Schizosaccharomyces pombe.* J. Cell Sci. *94*, 635–646.

Le Goff, X., Woollard, A., and Simanis, V. (1999). Analysis of the *cps1* gene provides evidence for a septation checkpoint in *Schizosaccharomyces pombe.* Mol. Gen. Genet. *262*, 163–172.

Letunic, I., Goodstadt, L., Dickens, N. J., Doerks, T., Schultz, J., Mott, R., Ciccarelli, F., Copley, R., Ponting, C., and Bork, P. (2002). Recent improvements to the SMART domain-based sequence annotation resource. Nucleic Acids Res. *30*, 242–244.

Liu, J., Tang, X., Wang, H., and Balasubramanian, M. K. (2000a). Bgs2p, a 1,3-b-glucan synthase subunit is essential for maturation of ascospore wall in *Schizosaccharomyces pombe.* FEBS Lett. *478*, 105–108.

Liu, J., Tang, X., Wang, H., Oliferenko, S., and Balasubramanian, M. K. (2002). The localization of the integral membrane protein Cps1p to the cell division site is dependent on the actomyosin ring and the septation-inducing network in *Schizosaccharomyces pombe.* Mol. Biol. Cell *13*, 989–1000.

Liu, J., Wang, H., and Balasubramanian, M. K. (2000b). A checkpoint that monitors cytokinesis in *Schizosaccharomyces pombe.* J. Cell Sci. *113*, 1223–1230.

Liu, X., Wang, H., Eberstadt, M., Schnuchel, A., Olejniczak, E. T., Meadows, R., and Fesik, S. W. (1998). NMR structure and mutagenesis of the N-terminal Dbl homology domain of the nucleotide exchange factor Trio. Cell *95*, 269–277.

Manners, D. J., and Meyer, M. T. (1977). The molecular structures of some glucans from the cell wall of *S. pombe.* Carbohydr. Res. *57*, 189–203.

Marks, J., and Hyams, J. S. (1985). Localization of F-actin through the cell division cycle of *Schizosaccharomyces pombe.* Eur. J. Cell Biol. *39*, 27–32.

Martin, S. G., McDonald, W. H., Yates, J., III, and Chang, F. (2005). Tea4p links microtubule plus ends with the formin For3p in the establishment of cell polarity. Dev. Cell *8*, 479–491.

Martin, V., García, B., Carnero, E., Duran, A., and Sanchez, Y. (2003). Bgs3p, a putative 1,3-b-glucan synthase subunit, is required for cell wall assembly in *Schizosaccharomyces pombe.* Eukaryot. Cell *2*, 159–169.

Martin, V., Ribas, J. C., Carnero, E., Durán, A., and Sánchez, Y. (2000). Bgs2+, a sporulation-specific glucan synthase homologue is required for proper ascospore wall maturation in fissión yeast. Mol. Microbiol. *38*, 308–321.

Mata, J., and Nurse, P. (1997). tea1 and the microtubular cytoskeleton are important for generating global spatial order within the fission yeast. Cell *89*, 939–950.

Mitchison, J. M., and Nurse, P. (1985). Growth in cell length in the fission yeast *Schizosaccharomyces pombe.* J. Cell Sci. *75*, 357–376.

Moreno, S., Klar, A., and Nurse, P. (1991). Molecular genetic analysis of fission yeast *Schizosaccharomyces pombe.* Methods Enzymol. *194*, 795–823.

Nakano, K., Arai, R., and Mabuchi, I. (1997). The small GTP binding protein Rho1 is a multifunctional protein that regulates actin localization, cell polarity, and septum formation in the fission yeast *Schizosaccharomyces pombe.* Genes Cells *2*, 679–694.

Nakano, K., Mutoh, T., and Mabuchi, I. (2001). Characterization of GTPase-activating proteins for the function of the Rho-family small GTPases in the fission yeast *Schizosaccharomyces pombe.* Genes Cells *6*, 1031–1042.

Osumi, M., Yamada, N., Kobori, H., Taki, A., Naito, N., Baba, M., and Nagatani, T. (1989). Cell wall formation in regenerating protoplast of *Schizosaccharomyces pombe*: study by high resolution, low voltage scanning electron microscopy. J. Electron. Microsc. *38*, 457–468.

Papadaki, P., Pizon, V., Onken, B., and Chang, E. (2002). Two ras pathways in fission yeast are differentially regulated by two ras guanine nucleotide exchange factors. Mol. Cell Biol. *22*, 4598–4606.

Pelham, R.J.J., and Chang, F. (2001). Role of actin polymerization and actin cables in actin-patch movement in *Schizosaccharomyces pombe*. Nat. Cell Biol. *3*, 235–244.

Reid, T., Furiyashiki, T., Ishizaki, T., Watanabe, G., Watanabe, N., Fujisawa, K., Morii, N., Madaule, P., and Nayumira, S. (1996). Rhotekin, a new putative target for Rho bearing homology to a serine/threonine kinase, PKN, and rhophilin in the rho-binding domain. J. Biol. Chem. *271*, 13556–13560.

Ren, X. D., Kiosses, W. B., and Schwartz, M. A. (1999). Regulation of the small GTP-binding protein Rho by cell adhesion and the cytoskeleton. EMBO J. *18*, 578–585.

Rossman, K. L., Channing, J. D., and Sondek, J. (2005). GEF means go: turning on Rho GTPases with guanine nucleotide-exchange factors. Nat. Rev. Mol. Cell Biol. *6*, 167–180.

Sayers, L. G., Katayama, S., Nakano, K., Mellor, H., Mabuchi, I., Toda, T., and Parker, P. J. (2000). Rho-dependence of *Schizosaccharomyces pombe* Pck2. Genes Cells *5*, 17–27.

Schmidt, A., and Hall, A. (2002). Guanine nucleotide exchange factors for Rho GTPases: turning on the switch. Genes Dev. *16*, 1587–1609.

Soisson, S. M., Nimnual, A. S., Uy, M., Bar-Sagi, D., and Kuriyan, J. (1998). crystal structure of the Dbl and pleckstrin homology domains from the human son of sevenless protein. Cell *95*, 259–268.

Tajadura, V., Garcia, B., Garcia, I., Garcia, P., and Sanchez, Y. (2004). *Schizosaccharomyces pombe* Rgf3p is a specific Rho1 GEF that regulates cell wall b-glucan biosynthesis through the GTPase Rho1p. J. Cell Sci. *117*, 6163–6174.

Toda, T., Shimanuki, M., and Yanagida, M. (1993). Two novel PKC-related genes of fission yeast are essential for cell viability and implicated in cell shape control. EMBO J. *12*, 1987–1995.

Verde, F., Mata, J., and Nurse, P. (1995). Fission yeast cell morphogenesis: identification of new genes and analysis of their role during the cell cycle. J. Cell Biol. *131*, 1529–1538.

Win, T. Z., Gachet, Y., Mulvihill, D. P., May, K. M., and Hyams, J. S. (2001). Two type V myosins with non-overlapping functions in the fission yeast *Schizosaccharomyces pombe*: Myo52 is concerned with growth polarity and cytokinesis, Myo 51 is a component of the cytokinetic actin ring. J. Cell Sci. *114*, 69–79.

Yarm, F., Sagot, I., and Pellman, D. (2001). The social life of actin and microtubules: interaction versus co-operation. Curr. Opi. Microbiol. *4*, 696–702.